J. Phys. Chem. A **2004,** *108,* 2103−2107

Extent of Delocalization of Vibrational Modes in Liquids as a Result of Competition between Diagonal Disorder and Off-Diagonal Coupling

Hajime Torii*,†

Department of Chemistry, School of Education, Shizuoka University, 836 Ohya, Shizuoka 422-8529, Japan

Received: November 26, 2003; In Final Form: January 19, 2004

The changes in the extent of delocalization of vibrational modes in liquids arising from the competition between diagonal disorder and off-diagonal coupling in the vibrational exciton picture are examined theoretically. Calculations of vibrational modes and polarized Raman spectra are carried out on a model liquid system, in which spherical particles interact with each other by the Lennard-Jones and dipole−dipole interactions, and a one-dimensional oscillator (representing a vibrational degree of freedom) with a transition dipole and a Raman tensor is buried in each particle. The diagonal disorder is assumed to be in a Gaussian form, and the transition dipole coupling is introduced as the off-diagonal coupling in the vibrational Hamiltonian. The magnitude of the Raman noncoincidence effect (NCE), which is the phenomenon that the vibrational frequency positions of the isotropic and anisotropic components of a Raman band do not coincide and is often used as an experimental measure of the delocalization of vibrational modes, is calculated. In addition, two theoretical measures of the delocalization of vibrational modes are introduced, and their changes with the thermodynamic state of the liquid, the diagonal disorder, and the strength of the off-diagonal coupling are examined. It is shown that the extent of delocalization of vibrational modes is correlated with the “NCE detectability”, defined as the ratio of the magnitude of the NCE and the isotropic or anisotropic Raman bandwidth. This result indicates that the extent of delocalization of vibrational modes in a vibrational band that shows the NCE may be estimated from the observed spectral profile of the band. The size of the space in which vibrational spectra can probe structural formation is also discussed.

1. Introduction

Vibrational dynamics and spectra of molecules in the liquid phase are affected by intermolecular interactions in various ways. In addition to vibrational frequency modulation and intramolecular mode mixing, direct coupling of vibrational modes of different molecules may occur in some cases. In the vibrational exciton picture, which is valid when the vibrational mode of interest in each molecule is sufficiently well separated in frequency from the other modes and hence intramolecular mode mixing can be safely neglected, the vibrational frequency modulation is called “diagonal” and the direct coupling of vibrational modes called “off-diagonal”, because they appear in the diagonal and off-diagonal terms, respectively, of the vibrational Hamiltonian constructed on the basis of the vibrational modes of individual molecules in the system.[1]

The effect of the off-diagonal vibrational coupling is most clearly seen in the resonant case, where the intrinsic frequencies of the interacting vibrational modes are sufficiently close to each other as compared with the magnitude of the coupling. In the frequency-domain picture, the resonant off-diagonal coupling gives rise to delocalization of vibrational modes. The Raman noncoincidence effect (NCE) of vibrational spectra,[2−5] the phenomenon that the vibrational frequency positions of the isotropic and anisotropic components of a Raman band do not coincide, is a clear indication of this delocalization of vibrational modes. In many cases, the vibrational coupling that gives rise to the NCE is determined by the transition dipole coupling (TDC) mechanism and hence is sensitive to the distance and relative orientation of the interacting molecules. Therefore, analysis of the NCE elucidates the structural formation in the liquid. In the time-domain picture, the resonant off-diagonal coupling gives rise to vibrational excitation transfer among molecules in the system. The ultrafast decay of transient infrared (IR) absorption anisotropy, which is observed for the OH stretching mode of liquid water,[6] occurs because of this vibrational excitation transfer. It has been shown that the decay rate of the transient IR absorption anisotropy in the time domain is related to the magnitude of the NCE in the frequency domain.[7]

In contrast, “diagonal” vibrational frequency modulation (or disorder in the diagonal terms of the vibrational Hamiltonian) is induced by local intermolecular interactions on individual molecules. It gives rise to inhomogeneous broadening (in the slow modulation regime) or dephasing (in the intermediate or fast modulation regime),[8] and is seen more or less in essentially all the vibrational bands. In the presence of resonant off-diagonal vibrational coupling, the effect of this diagonal disorder is to make those vibrational motions partially off-resonant and hence to reduce the extent of delocalization of vibrational modes. In this sense, the diagonal disorder competes with the off-diagonal vibrational coupling. Therefore, to estimate the extent of delocalization of vibrational modes from observed vibrational spectra and to clarify how large is the space in which vibrational spectra can probe structural formation, it is important to see the changes in the vibrational spectra and in the delocalization of vibrational modes as a result of the competition between the diagonal and off-diagonal effects.

---

* Address correspondence to the author at the following: phone +81-54-238-4624; fax +81-54-237-3354; e-mail torii@ed.shizuoka.ac.jp.

† Also a visiting associate professor at the Department of Theoretical Studies, Institute for Molecular Science, Okazaki 444-8585, Japan.

10.1021/jp037603s CCC: $27.50

In the present study, this point is examined quantitatively by the calculations on a model liquid system, in which spherical particles interact with each other by the Lennard-Jones and dipole−dipole interactions (Stockmayer fluid),[9] and a one-dimensional oscillator (representing a vibrational degree of freedom) with a transition dipole and a Raman tensor is buried in each particle.[7] A study on this kind of simple liquid is needed to found a basis that may be used as a reference in the studies on the effects of complexities arising from the molecular aspects of real liquids, and to obtain a unified view. We introduce two quantities that represent the extent of delocalization of vibrational modes, and examine their changes, as well as the corresponding changes in the Raman spectral profiles, with the thermodynamic state of the liquid, the diagonal disorder, and the strength of the off-diagonal coupling. It is shown that the extent of delocalization of vibrational modes is correlated with the "NCE detectability", defined as the ratio of the magnitude of the NCE and the isotropic or anisotropic Raman bandwidth. The meaning of this result in the interpretation of observed Raman spectra is discussed.

2. Computational Procedure

The vibrational modes and the polarized Raman spectra of the model liquid were calculated by the MC/TDC method[1,5] in the vibrational exciton picture, where the liquid structures were obtained by the Monte Carlo (MC) method and the off-diagonal coupling constants were determined by the transition dipole coupling (TDC) mechanism. According to this TDC mechanism, the off-diagonal coupling constant between molecules j and k is given as

$$F_{jk} = \frac{\left(\frac{\partial \boldsymbol{\mu}_j}{\partial q_j}\right)\cdot\left(\frac{\partial \boldsymbol{\mu}_k}{\partial q_k}\right) - 3\left[\left(\frac{\partial \boldsymbol{\mu}_j}{\partial q_j}\right)\cdot\mathbf{n}_{jk}\right]\left[\left(\frac{\partial \boldsymbol{\mu}_k}{\partial q_k}\right)\cdot\mathbf{n}_{jk}\right]}{{r_{jk}}^3} \qquad (1)$$

where $\partial\boldsymbol{\mu}_j/\partial q_j$ and $\partial\boldsymbol{\mu}_k/\partial q_k$ are the dipole derivatives of the modes in molecules j and k, $\mathbf{n}_{jk}$ is the unit vector along the line connecting the two molecules, and r_{jk} is the distance between the two molecules. This formula is derived as the second derivative (with respect to q_j and q_k) of the dipole−dipole interaction energy between the two molecules. It is easily recognized that this off-diagonal coupling constant is sensitive to the distance and relative orientation of the interacting molecules.

The interparticle (intermolecular) interaction parameters used for calculating the liquid structures were set as $\sigma = 4.2$ Å (nearly equal to the hard sphere diameter of 4.185 Å estimated[10] for simulating liquid acetone), $\epsilon = 150$ K, and $\mu = 3.097$ D ($\mu^* \equiv \mu(\epsilon\sigma^3)^{-1/2} = 2.5$). Four thermodynamic states with (T^*, ρ^*) = (2.0, 0.9), (4.0, 0.9), (4.0, 0.45), and (4.0, 0.2) were considered, where T^* and ρ^* were defined as $T^* \equiv T/\epsilon$ and $\rho^* \equiv \rho\sigma^3$. Of these four states, the first one is in the isotropic liquid region and the other three are in the supercritical fluid region (in the sense that the temperature is higher than that of the critical point), according to the phase diagram obtained by Stevens and Grest.[11] Since the orientational order in the liquid is mainly controlled by the quantity μ^2/kT,[3,4,10] the changes in the spectral profiles, etc., with temperature are related more or less to those with the molecular dipole moment with regard to the orientational order in the liquid. Therefore, the states treated in the present simulations are related to various situations of liquid systems. Although there is only one state in the isotropic liquid region in the above setting of parameters, the state with (T^*, ρ^*) = (4.0, 0.9) is rather liquid-like because of the high number density. The results expected at intermediate temperatures in the isotropic liquid region may therefore be obtained by interpolation. It should also be noted that the variation of the results as a function of ρ^* has some relation with the concentration dependence observed in binary mixtures of real systems,[12−14] because the orientational order and the vibrational coupling are determined, as far as the solvent is inert, by the interactions among "active" molecules.

MC simulations were carried out on a system consisting of $N = 512$ particles in a cubic cell with the Metropolis sampling scheme and the periodic boundary condition.[15,16] The system was equilibrated for the first 1.2×10^7 steps (equivalent to 2.3×10^4 MC cycles), and 4000 configurations were extracted as liquid structure samples from the subsequent 2×10^9 steps (equivalent to 3.9×10^6 MC cycles).

For each of these configurations of liquid structure, the force constant matrix (**F** matrix) was constructed for the vibrational degrees of freedom buried in the particles. The diagonal elements of the **F** matrix were assumed to be distributed in a Gaussian form with a standard deviation σ_f in the range of 0.00−0.02 mdyn Å^{-1} amu^{-1} around the average value of 1.737 mdyn Å^{-1} amu^{-1}. The latter value is equal to that used for the C=O stretching mode of neat liquid acetone[13,17] and corresponds to the vibrational frequency of 1717 cm^{-1}. The dipole derivatives $\partial\boldsymbol{\mu}/\partial q$, the origin of the off-diagonal vibrational coupling in the TDC mechanism (eq 1), of the oscillators of all the particles in the system were assumed to have a common magnitude in the range of 0.100−2.626 D Å^{-1} amu$^{-1/2}$, and the direction of $\partial\boldsymbol{\mu}/\partial q$ in each particle was assumed to be parallel to the permanent dipole, which was set as the principal axis of the particle. (Note that the value of $|\partial\boldsymbol{\mu}/\partial q|$ of the C=O stretching mode of acetone derived from its IR intensity is 2.08 D Å^{-1} amu$^{-1/2}$ (refs 5 and 13), indicating that the above range of $|\partial\boldsymbol{\mu}/\partial q|$ in the present calculations is sufficiently reasonable.) The Raman tensors of the oscillators of all the particles in the system were also assumed to have a common magnitude and to be uniaxial with a nonzero element only in the direction of the principal axis. The **F** matrix thus constructed was diagonalized to obtain the vibrational modes of the liquid. The polarized Raman spectrum was calculated, as the statistical average over the 4000 configurations of liquid structure, by using those vibrational modes and the Raman tensors. The values of σ_f and $|\partial\boldsymbol{\mu}/\partial q|$ were varied in the ranges described above, and the calculations of the vibrational modes and the polarized Raman spectrum were carried out for each set of these values.

The following two quantities were calculated to examine the extent of delocalization of vibrational modes. (1) The vibrational amplitude correlation function (VACF) is defined as

$$\zeta(r) = \frac{\langle \sum_{j,k} (\sum_m |c_{jm}c_{km}|)\ \delta(r - r_{jk})\rangle}{\langle \sum_{j,k} \delta(r - r_{jk})\rangle} \qquad (2)$$

where c_{jm} is the normalized vibrational amplitude of the jth molecule (particle) in the mth mode, r_{jk} is the intermolecular distance between molecules j and k, and the brackets, $\langle\ \rangle$, stand for the statistical average. This quantity represents the correlation of vibrational amplitudes as a function of intermolecular distance, and is in the range between 0 (no correlation) and 1

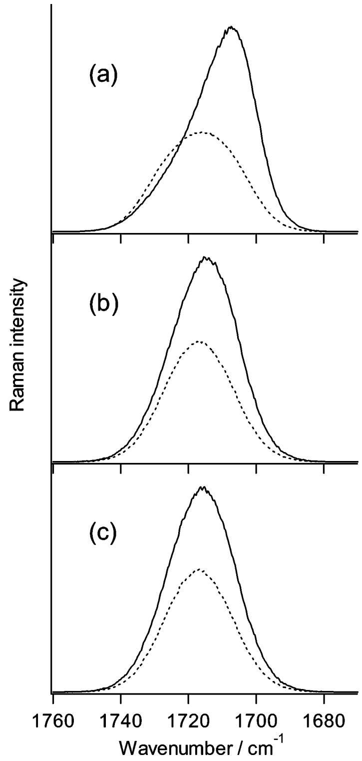

Figure 1. The polarized Raman spectra calculated for the state (T^*, ρ^*) = (4.0, 0.45) with the values of $\sigma_f = 0.02$ mdyn Å^{-1} amu^{-1} and (a) $|\partial\boldsymbol{\mu}/\partial q| = 2.0$ D Å^{-1} amu$^{-1/2}$, (b) $|\partial\boldsymbol{\mu}/\partial q| = 1.0$ D Å^{-1} amu$^{-1/2}$, and (c) $|\partial\boldsymbol{\mu}/\partial q| = 0.707$ D Å^{-1} amu$^{-1/2}$. The isotropic and anisotropic components are drawn in solid and broken lines, respectively.

(full correlation).[18] (2) The frequency-dependent participation ratio is defined as

$$\eta(\omega) = \frac{\langle \sum_m (\sum_j c_{jm}{}^4)^{-1}\, \delta(\omega - \omega_m)\rangle}{\langle \sum_m \delta(\omega - \omega_m)\rangle} \tag{3}$$

where ω_m is the vibrational frequency of the mth mode. This quantity represents the average extent of delocalization of the modes at the specified frequency, and is equal to 1 if the modes at the specified frequency are completely localized and N if they are delocalized uniformly over N molecules.[19-23]

All the calculations described above were carried out with our original programs on a Fujitsu VPP5000 supercomputer at the Research Center for Computational Science of the Okazaki National Research Institutes.

3. Results and Discussion

The polarized Raman spectra calculated for the state (T^*, ρ^*) = (4.0, 0.45) with the values of $\sigma_f = 0.02$ mdyn Å^{-1} amu^{-1} and $|\partial\boldsymbol{\mu}/\partial q| = 2.0$, 1.0, and 0.707 D Å^{-1} amu$^{-1/2}$ are shown in Figure 1.[24] In the spectrum calculated with $|\partial\boldsymbol{\mu}/\partial q| = 2.0$ D Å^{-1} amu$^{-1/2}$ shown in Figure 1a, it is clearly seen that the isotropic Raman component is located at a lower frequency position than the anisotropic component, i.e., the NCE defined as $\nu_{\text{NCE}} \equiv \nu_{\text{aniso}} - \nu_{\text{iso}}$ is positive, as in the case of the C=O stretching band of liquid acetone[12,25-28] and other related liquids.[25,29-31] The reason for the asymmetry of the isotropic Raman component is discussed, in the case of the C=O stretching band of liquid acetone, in ref 17. As the value of $|\partial\boldsymbol{\mu}/\partial q|$ decreases, the magnitude of NCE gets smaller. A positive NCE is also (but barely) noticeable in the spectrum calculated with $|\partial\boldsymbol{\mu}/\partial q| = 1.0$ D Å^{-1} amu$^{-1/2}$ shown in Figure 1b. In the spectrum calculated with $|\partial\boldsymbol{\mu}/\partial q| = 0.707$ D Å^{-1} amu$^{-1/2}$ shown in Figure 1c, the NCE is also positive, but it is so small (0.64 cm^{-1} calculated from the first moments) as compared with the isotropic and anisotropic bandwidths ($\sigma_{\text{iso}} \cong \sigma_{\text{aniso}} = 9.9$ cm^{-1}, where σ_{iso} and σ_{aniso} are the standard deviation of the spectral intensity distribution of the isotropic and anisotropic Raman bands, respectively) that the NCE is not easily recognized. The magnitude of NCE also depends on the thermodynamic state, because it is related to the local structural order in the liquid. With $\sigma_f = 0.02$ mdyn Å^{-1} amu^{-1} and $|\partial\boldsymbol{\mu}/\partial q| = 2.0$ D Å^{-1} amu$^{-1/2}$, the values of NCE are calculated to be 9.6, 8.1, 5.1, and 3.0 cm^{-1} for the states (T^*, ρ^*) = (2.0, 0.9), (4.0, 0.9), (4.0, 0.45), and (4.0, 0.2), respectively. In contrast, the magnitude of NCE does not depend on the value of σ_f, although the isotropic and anisotropic Raman bandwidths are (of course) strongly dependent on it.

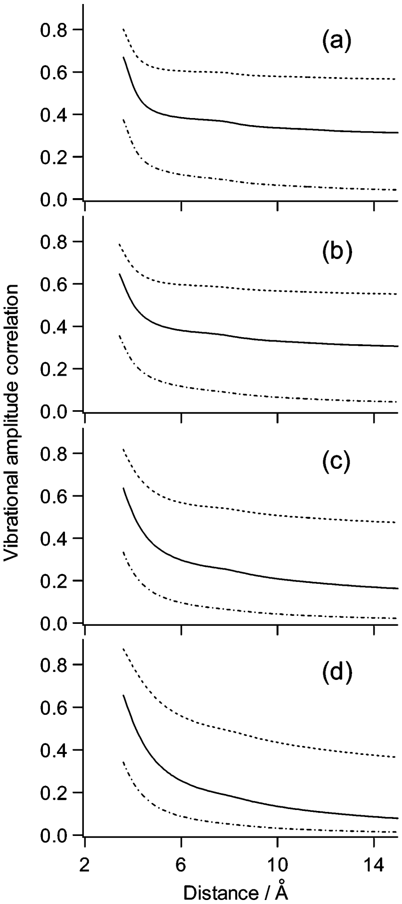

Figure 2. The VACFs $\zeta(r)$ (defined by eq 2) calculated for the state (a) (T^*, ρ^*) = (2.0, 0.9), (b) (T^*, ρ^*) = (4.0, 0.9), (c) (T^*, ρ^*) = (4.0, 0.45), and (d) (T^*, ρ^*) = (4.0, 0.2). For each state, $\zeta(r)$ is calculated with three sets of values of (σ_f/mdyn Å^{-1} amu^{-1}, $|\partial\boldsymbol{\mu}/\partial q|$/D Å^{-1} amu$^{-1/2}$) = (0.00, 2.0), (0.02, 2.0), and (0.02, 1.0), and drawn in broken, solid, and dot−dashed lines, respectively.

The VACFs $\zeta(r)$ calculated for the four thermodynamic states with the values of (σ_f/mdyn Å^{-1} amu^{-1}, $|\partial\boldsymbol{\mu}/\partial q|$/D Å^{-1} amu$^{-1/2}$) = (0.00, 2.0), (0.02, 2.0), and (0.02, 1.0) are shown in Figure 2. In all cases, the value of $\zeta(r)$ gets smaller as the intermolecular distance r increases. Comparing the results obtained for the four thermodynamic states, it is seen that the decrease of the value of $\zeta(r)$ as a function of r becomes more significant at a lower density and (although slightly) at a higher temperature. At each state, the value of $\zeta(r)$ becomes smaller as the diagonal disorder σ_f increases and (for a nonzero value of σ_f) as the magnitude of

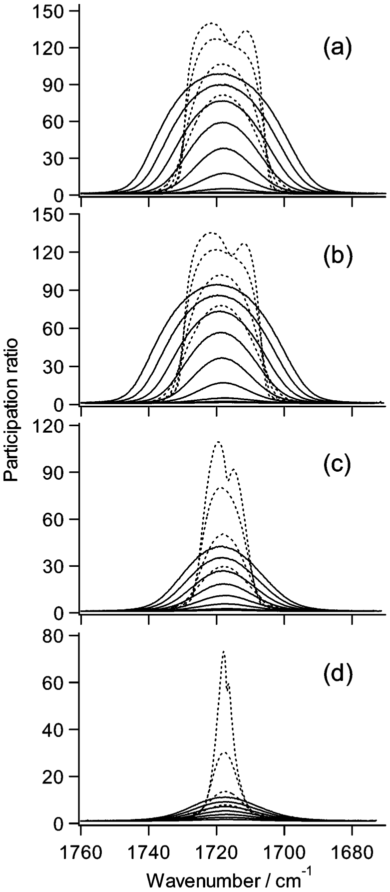

Figure 3. The frequency-dependent participation ratios $\eta(\omega)$ (defined by eq 3) calculated for the state (a) (T^*, ρ^*) = (2.0, 0.9), (b) (T^*, ρ^*) = (4.0, 0.9), (c) (T^*, ρ^*) = (4.0, 0.45), and (d) (T^*, ρ^*) = (4.0, 0.2). For each state, the solid lines show the values calculated with σ_f = 0.02 mdyn Å^{-1} amu^{-1} and $|\partial\boldsymbol{\mu}/\partial q|$ = 2.626, 2.449, 2.236, 2.0, 1.732, 1.414, 1.0, 0.707, and 0.5 D Å^{-1} amu$^{-1/2}$ (from top to bottom), and the broken lines show the values calculated with $|\partial\boldsymbol{\mu}/\partial q|$ = 2.0 D Å^{-1} amu$^{-1/2}$ and σ_f = 0.000, 0.005, 0.010, and 0.015 mdyn Å^{-1} amu^{-1} (from top to bottom).

dipole derivative $|\partial\boldsymbol{\mu}/\partial q|$ decreases. For example, for the set of parameters that gives rise to the Raman spectrum with a significant magnitude of NCE shown in Figure 1a, the value of $\zeta(r)$ is ~0.21 at r = 10.0 Å as shown in a solid line in Figure 2c, indicating that the vibrational amplitudes between the molecules at this distance apart are correlated with each other to an intermediate extent. However, for the situation corresponding to the Raman spectrum shown in Figure 1b that shows a barely noticeable NCE, the value of $\zeta(r)$ is ~0.04 at r = 10.0 Å as shown in a dot−dashed line in Figure 2c, indicating that the correlation of the molecular vibrations is limited to a small space.

In Figure 3 are shown the frequency-dependent participation ratios $\eta(\omega)$ calculated for the four thermodynamic states with σ_f = 0.02 mdyn Å^{-1} amu^{-1} and $|\partial\boldsymbol{\mu}/\partial q|$ in the range of 2.626−0.500 D Å^{-1} amu$^{-1/2}$ (solid lines) and with $|\partial\boldsymbol{\mu}/\partial q|$ = 2.0 D Å^{-1} amu$^{-1/2}$ and σ_f in the range of 0.015−0.000 mdyn Å^{-1} amu^{-1} (broken lines). For all sets of parameters, the value of $\eta(\omega)$ is large around the band center and small on the wing. The peak height gets larger as $|\partial\boldsymbol{\mu}/\partial q|$ increases (for a fixed σ_f) and as σ_f decreases (for a fixed $|\partial\boldsymbol{\mu}/\partial q|$). Comparing the results obtained for the four thermodynamic states, it is seen that a larger peak height is obtained at a higher density and at a lower temperature. For the cases with small values of σ_f, the bandwidth of $\eta(\omega)$ also changes noticeably with the thermo-dynamic state, because the band broadening arises not only from the diagonal disorder but also from the off-diagonal vibrational coupling,[5] and the latter varies with the liquid structure even for the same value of $|\partial\boldsymbol{\mu}/\partial q|$, as noticed also from the dependence of the magnitude of NCE on the thermodynamic state of the liquid illustrated above.

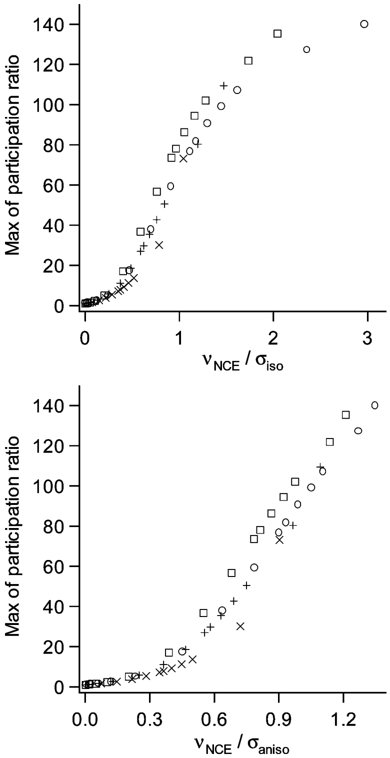

Figure 4. The values of max{$\eta(\omega)$} [the peak height of $\eta(\omega)$ shown in Figure 3] plotted against the NCE detectability (defined as ν_{NCE}/σ_{iso} and ν_{NCE}/σ_{aniso}): ○, (T^*, ρ^*) = (2.0, 0.9); □, (T^*, ρ^*) = (4.0, 0.9); +, (T^*, ρ^*) = (4.0, 0.45); ×, (T^*, ρ^*) = (4.0, 0.2). See the caption for Figure 3 for the detailed setting of σ_f and $|\partial\boldsymbol{\mu}/\partial q|$.

As described in Section 2, $\eta(\omega)$ is a measure of the number of molecules over which the vibrational modes are delocalized. For the situation that corresponds to Figure 1a and the solid line in Figure 2c showing a significant magnitude of NCE, the peak height of $\eta(\omega)$ is calculated as max{$\eta(\omega)$} = 18.6, suggesting that the vibrational modes are delocalized to the second shell of neighboring molecules and partially to the third shell as well. However, for the situation that corresponds to Figure 1b and the dot−dashed line in Figure 2c showing a barely noticeable NCE, we obtain max{$\eta(\omega)$} = 2.6, indicating that the vibrational modes are delocalized only over a few molecules.

Considering that the vibrational modes do not change when the values of σ_f and $|\partial\boldsymbol{\mu}/\partial q|^2$ are varied by the same ratio because of the similarity (in a mathematical sense) of the vibrational Hamiltonian, it may be reasonable to consider that the extent of delocalization of vibrational modes is related to the ratio of the magnitude of NCE and the Raman bandwidth, which is a dimensionless quantity.[32] This ratio may be called "NCE detectability" in the sense that, aside from the instrumental problem in the experiment, the NCE is more easy to detect as its magnitude gets larger *compared with the bandwidth*. The plot of the peak height of $\eta(\omega)$ against the ratio of the magnitude of NCE and the standard deviation of the isotropic and anisotropic Raman intensity distributions (ν_{NCE}/σ_{iso} and ν_{NCE}/σ_{aniso}) is shown in Figure 4. It is clearly seen that the peak height of $\eta(\omega)$ has a good correlation with both ν_{NCE}/σ_{iso} and ν_{NCE}/σ_{aniso}.

This result indicates that the extent of delocalization of vibrational modes in a vibrational band that shows the NCE may be estimated from the observed spectral profile of the band. The values of ν_{NCE}/σ_{iso} and ν_{NCE}/σ_{aniso} of some vibrational bands of real liquids fall in the range that, according to Figure 4, suggests extensive delocalization of vibrational modes; for example, in the case of the C=O stretching band of liquid acetone, the values of these two quantities are estimated as $\nu_{NCE}/\sigma_{iso} \cong 1.44$ and $\nu_{NCE}/\sigma_{aniso} \cong 0.60$ from the observed band profiles shown in the previous studies.[12,13,17] Of course, vibrational band broadening in real liquids arises not only from diagonal disorder (or local vibrational frequency fluctuation) and off-diagonal vibrational coupling but also from vibrational population relaxation, and may be affected by motional narrowing and (for anisotropic Raman bands) rotational relaxation.[33] In addition, the intermolecular interactions in real liquids may be more complicated than the simple dipole−dipole and Lennard-Jones interactions, and the form of the diagonal disorder may deviate from a Gaussian distribution and may be correlated with the off-diagonal coupling constants. However, it is expected that *a rough estimate* of the extent of delocalization may be obtained from the observed NCE detectability regardless of these limitations. The effects of various complexities arising from the molecular aspects of real liquids deserve future studies.

4. Summary

In the present study, we have examined the changes in the extent of delocalization of vibrational modes in liquids arising from the competition between diagonal disorder and off-diagonal coupling by the calculations on a model liquid system. It has been shown that the extent of delocalization of vibrational modes is correlated with the NCE detectability defined as the ratio of the magnitude of the NCE and the isotropic or anisotropic Raman bandwidth (ν_{NCE}/σ_{iso} or ν_{NCE}/σ_{aniso}). For the situation that shows a significant magnitude of NCE, the vibrational modes are delocalized over many molecules, so that the vibrational amplitudes are correlated between molecules at a distance $r \sim 10$ Å or longer. It has been suggested that the extent of delocalization of vibrational modes in a vibrational band that shows the NCE may be roughly estimated from the observed spectral profile of the band.

The results of the present study indicate that vibrational spectra may probe structural formation on the scale of more than 10 Å in the case where the off-diagonal vibrational coupling is significantly large as compared with the magnitude of diagonal disorder. Although the magnitude of the NCE of some vibrational modes of real liquids is determined essentially by the liquid structure within ∼6 Å,[10,13,14,34] it is considered to be due to the structural disorder of the liquid, taking into account the wavy form of the integrated second-order pair distribution functions [denoted as $H_D(r)$] obtained for those liquids. For materials with well-ordered arrangement of molecules (or vibrational units), vibrational spectra may be sensitive to structural formation on such a long length scale. Studies on this point will also provide insight into the intermolecular vibrational excitation transfer in large-scale molecular systems.

Acknowledgment. This study was supported by a Grant-in-Aid for Scientific Research from the Ministry of Education, Culture, Sports, Science, and Technology.

References and Notes

(1) Torii, H. In *Novel Approaches to the Structure and Dynamics of Liquids*: *Experiments*, *Theories and Simulations*; Samios, J., Durov, V. A., Eds.; Kluwer: Dordrecht, The Netherlands, in press.

(2) Fini, G.; Mirone, P.; Fortunato, B. *J. Chem. Soc., Faraday Trans. 2* **1973**, *69*, 1243.

(3) (a) Wang, C. H.; McHale, J. *J. Chem. Phys.* **1980**, *72*, 4039. (b) McHale, J. L. *J. Chem. Phys.* **1981**, *75*, 30.

(4) Logan, D. E. *Chem. Phys.* **1986**, *103*, 215.

(5) Torii, H.; Tasumi, M. *J. Chem. Phys.* **1993**, *99*, 8459.

(6) Woutersen, S.; Bakker, H. J. *Nature* **1999**, *402*, 507.

(7) Torii, H. *Chem. Phys. Lett.* **2000**, *323*, 382.

(8) Kubo, R. *Adv. Chem. Phys.* **1969**, *15*, 101.

(9) Hansen, J.-P.; McDonald, I. R. *Theory of Simple Liquids*; Academic Press: London, UK, 1986.

(10) Torii, H. *J. Mol. Struct.* (*THEOCHEM*) **1994**, *311*, 199.

(11) Stevens, M. J.; Grest, G. S. *Phys. Rev. E* **1995**, *51*, 5976.

(12) Musso, M.; Giorgini, M. G.; Döge, G.; Asenbaum, A. *Mol. Phys.* **1997**, *92*, 97.

(13) Torii, H.; Musso, M.; Giorgini, M. G.; Döge, G. *Mol. Phys.* **1998**, *94*, 821.

(14) Musso, M.; Torii, H.; Ottaviani, P.; Asenbaum, A.; Giorgini, M. G. *J. Phys. Chem. A* **2002**, *106*, 10152.

(15) Metropolis, N.; Rosenbluth, A. W.; Rosenbluth, M. N.; Teller, A. H.; Teller, E. *J. Chem. Phys.* **1953**, *21*, 1087.

(16) Allen, M. P.; Tildesley, D. J. *Computer Simulation of Liquids*; Oxford University Press: Oxford, UK, 1989.

(17) Musso, M.; Torii, H.; Giorgini, M. G.; Döge, G. *J. Chem. Phys.* **1999**, *110*, 10076.

(18) From $\sum_m(|c_{jm}| - |c_{km}|)^2 \geq 0$ and $\sum_m c_{jm}{}^2 = \sum_m c_{km}{}^2 = 1$, we obtain $\sum_m |c_{jm}c_{km}| \leq 1$. The equality in the last equation holds if and only if $|c_{jm}| = |c_{km}|$ for all m.

(19) Bell, R. J.; Dean, P. *Discuss. Faraday Soc.* **1970**, *50*, 55.

(20) Thouless, D. J. *Phys. Rep.* **1974**, *13*, 93.

(21) Weaire, D.; Williams, A. R. *J. Phys. C*: *Solid State Phys.* **1977**, *10*, 1239.

(22) Evensky, D. A.; Scalettar, R. T.; Wolynes, P. G. *J. Phys. Chem.* **1990**, *94*, 1149.

(23) A different definition of the frequency-dependent (inverse) participation ratio is described in: Piryatinski, A.; Asher, S. A.; Mukamel, S. *J. Phys. Chem. A* **2002**, *106*, 3524.

(24) The Raman spectra corresponding to specific configurations of the incident and scattered light may be easily constructed from the spectra of the isotropic and anisotropic components.

(25) Fini, G.; Mirone, P. *J. Chem. Soc., Faraday Trans. 2* **1974**, *70*, 1776.

(26) Schindler, W.; Sharko, P. T.; Jonas, J. *J. Chem. Phys.* **1982**, *76*, 3493.

(27) Giorgini, M. G.; Fini, G.; Mirone, P. *J. Chem. Phys.* **1983**, *79*, 639.

(28) Dybal, J.; Schneider, B. *Spectrochim. Acta A* **1985**, *41*, 691.

(29) Thomas. H. D.; Jonas, J. *J. Chem. Phys.* **1989**, *90*, 4144.

(30) Shelley, V. M.; Yarwood, J. *Chem. Phys.* **1989**, *137*, 277.

(31) Mortensen, A.; Faurskov Nielsen, O.; Yarwood, J.; Shelley, V. *J. Phys. Chem.* **1994**, *98*, 5221.

(32) By introducing this dimensionless quantity, the result does not depend on the assumed value of the average diagonal force constant (1.737 mdyn Å^{-1} amu^{-1}) as far as this value is significantly larger than the magnitude of σ_f and the off-diagonal force constants.

(33) Torii, H. *J. Phys. Chem. A* **2002**, *106*, 3281.

(34) Torii, H. *J. Phys. Chem. A* **1999**, *103*, 2843.